

# Stability of universal properties against perturbations of the Markov Chain Monte Carlo algorithm

Matteo Bacci<sup>1</sup> and Claudio Bonati<sup>1</sup>

<sup>1</sup>*Dipartimento di Fisica dell'Università di Pisa and INFN Sezione di Pisa, Largo Pontecorvo 3, I-56127 Pisa, Italy*

(Dated: June 24, 2025)

We numerically investigate the stability of universal properties at continuous phase transitions against perturbations of the Markov Chain Monte Carlo algorithm used to simulate the system. We consider the three dimensional XY model as test bed, and both local (single site Metropolis) and global (single cluster) updates, introducing deterministic truncation-like perturbations and stochastic perturbations in the acceptance probabilities. In (almost) all the cases we find a remarkable stability of the universal properties, even against large perturbations of the Markov Chain Monte Carlo algorithm, with critical exponents and scaling curves consistent with those of the standard XY model within statistical uncertainties.

## I. INTRODUCTION

Since only few statistical models can be analytically solved, and mainly in two dimensions (see, e. g., [1–3]), in statistical mechanics we often have to resort to numerical simulations. The Markov Chain Monte Carlo (MCMC) method is one of the most commonly used approaches to numerically investigate the equilibrium properties of statistical systems [4–9], since it provides stochastically exact estimates of average values whenever its application is not hindered by the presence of a sign problem [10–13].

Two different groups of applications of the MCMC method in statistical physics can be naturally identified. In some cases we know exactly (or at least with a high degree of accuracy) the microscopic details of the system we are interested in, and our aim is to estimate some macroscopic properties of direct physical interest, like, e. g., the value of the specific heat for a given temperature or the details of the phase diagram. In other cases the properties we want to study are not peculiar of a single physical model, but characterize a whole class of systems, the typical example being that of universal properties at continuous phase transitions [14–18]. Since the critical behavior emerging close to a continuous phase transition nonperturbatively defines a quantum field theory (QFT), all numerical studies of QFT effectively fall in this second category of applications [19–23].

Since double (or higher) precision has become commonplace, it seems that little concern has been shown about the possibility that machine precision limitations might significantly influence the numerical results of MCMC simulations. Some theoretical results regarding the behavior of the MCMC algorithm in the presence of truncation errors have been obtained in Refs. [24, 25], which, loosely speaking, state that the MCMC algorithm is stable against this type of perturbation. This means that the perturbed Markov chain still converges to a unique invariant probability distribution, and this probability distribution is “close” to that of the unperturbed Markov chain. Similar conclusions have been reached for stochastic perturbations of the MCMC algorithm, the so called Markov chains in random environment, which

have also been considered in the mathematical literature, see, e. g., [26, 27]. Stochastic perturbations are relevant both for quantum computing applications [28–32] and for rounding errors in architectures for which thread scheduling is non-deterministic.

These theoretical results show that the MCMC approach is robust with respect to a large class of perturbations as far as we consider the first class of applications introduced above, however they seem to be of little use to understand whether universal properties are stable or not against perturbations of the MCMC algorithm. Since continuous phase transitions correspond to points of the phase diagram where the free energy is non-analytic in the thermodynamic limit, the closeness of the invariant probability distribution function of the perturbed MCMC to that of the exact MCMC, for fixed volume, is not enough to guarantee that the two Markov chains display the same critical behavior.

A simple example can be useful to clearly understand this point: if we consider the perturbation of the MCMC used to sample an Ising model obtained by introducing an external magnetic field  $h$ , it is immediate to see that, at fixed lattice volume, the probability distribution function of the  $h \neq 0$  model is arbitrarily close to that of the  $h = 0$  model as far as we keep  $|h|$  small enough. On the other hand, for whatever small but non-vanishing value of  $|h|$  there is no phase transition if we keep  $h$  fixed and perform the thermodynamic limit, although very large lattices may be needed to notice this fact in an actual numerical simulation.

The aim of the present paper is to systematically investigate, by means of numerical simulations, the effect that perturbations of the MCMC algorithm have on the critical behavior of a classical statistical model. In particular we will use the three dimensional XY model as test bed (see, e. g., [33–41] for some determinations of its critical properties).

We consider locally reversible updates, i. e. satisfying the detailed balance principle, since these are so far the most commonly adopted ones, see however [42] for a recent review on non-reversible update schemes. Even assuming reversibility there is however still much freedom

in the implementation of a MCMC algorithm to sample the configuration space of a given classical statistical system, and only in few cases it is possible to associate the Monte Carlo evolution to a physical real-time evolution (see, e. g., [43, 44] for the corresponding critical dynamics). It is thus possible that some implementations turn out to be more robust than others. For this reason we study both perturbations of the single site Metropolis update [45] and of the single cluster update [46], considering deterministic and stochastic perturbations in both the cases. It would obviously be possible to add also a microcanonical update, thus obtaining an overrelaxed update scheme [47], however we prefer to consider just the simplest local or cluster updates in order to simplify the interpretation of the numerical results.

The paper is organized as follows: in Sec. II we introduce the MCMC algorithms used to sample the configurations of the three dimensional XY model, and describe the perturbations of these algorithms considered in the present work. In Sec. III we define the main observables used to investigate the critical behavior and recall some fundamental facts about Finite Size Scaling (FSS), then we discuss the numerical results obtained using the perturbed MCMC algorithms. Finally, in Sec IV, we draw our conclusions.

## II. THE XY MODEL AND THE MCMC PERTURBATIONS STUDIED

As anticipated in the introduction, we use the three dimensional XY model as test bed to investigate how perturbations of the MCMC algorithm affect the critical behavior of a classical spin system. The three dimensional XY model is obtained by associating a two dimensional vector  $\mathbf{s}_n$ , normalized in such a way that  $|\mathbf{s}_n| = 1$ , to each site  $\mathbf{n}$  of a three dimensional lattice. The Hamiltonian of the system is

$$H[\{\mathbf{s}_n\}] = -J \sum_{\langle \mathbf{n}, \mathbf{k} \rangle} \mathbf{s}_n \cdot \mathbf{s}_k, \quad (1)$$

where the notation  $\langle \ , \ \rangle$  is used to specify that the sum extends on all neighboring sites of the lattice, and the partition function is thus given by ( $\beta = 1/(k_B T)$ )

$$Z = \sum_{\{\mathbf{s}_n\}} e^{-\beta H[\{\mathbf{s}_n\}]}. \quad (2)$$

We use the ferromagnetic XY model ( $J > 0$ ), and by measuring the coupling  $J$  in units of the temperature we can effectively set  $J = 1$  in the Hamiltonian. As usual we perform simulations using cubic lattices with periodic boundary conditions, and we denote by  $L$  the linear extent of the lattice.

We consider two different update schemes: the single site Metropolis update and the single cluster update. In the single site Metropolis update we sweep through the lattice in lexicographic order, we generate a new random

vector  $\mathbf{s}^{(\text{trial})}$ , and accept the update  $\mathbf{s}_n \rightarrow \mathbf{s}^{(\text{trial})}$  with probability

$$P = \min(1, e^{-\beta \Delta E}), \quad (3)$$

where  $\Delta E = H(\{\mathbf{s}_n \rightarrow \mathbf{s}^{(\text{trial})}\}) - H(\{\mathbf{s}_n\})$  is the energy change of the configuration induced by the substitution  $\mathbf{s}_n \rightarrow \mathbf{s}^{(\text{trial})}$ . In the single cluster update [46] we instead randomly select the direction  $\mathbf{v}$  ( $|\mathbf{v}| = 1$ ) in the spins two dimensional space, and we denote by  $R_{\mathbf{v}}(\mathbf{s})$  the reflection with respect to plane orthogonal to  $\mathbf{v}$ :

$$R_{\mathbf{v}}(\mathbf{s}) = \mathbf{s} - 2(\mathbf{v} \cdot \mathbf{s})\mathbf{v}. \quad (4)$$

The real update starts by randomly picking a site  $\mathbf{n}$  and performing the substitution  $\mathbf{s}_n \rightarrow R_{\mathbf{v}}(\mathbf{s}_n)$ . The site  $\mathbf{n}$  is then used as a seed to build a cluster, by recursively adding neighboring sites with probability

$$P(\mathbf{s}_i, \mathbf{s}_o) = 1 - \exp\left(\min[0, 2\beta(\mathbf{s}_i \cdot \mathbf{v})(\mathbf{s}_o \cdot \mathbf{v})]\right), \quad (5)$$

where  $\mathbf{s}_i$  is a spin already included in the cluster and  $\mathbf{s}_o$  is a next-neighbor of the spin  $\mathbf{s}_i$  not yet included in the cluster. The spin of any site added to the cluster is updated using the reflection  $R_{\mathbf{v}}$ , and the construction goes on until an iteration is reached in which no further sites are added to the cluster.

With the purpose of investigating the stability of the XY critical properties against perturbations of the MCMC algorithm, we now introduce some deterministic and stochastic perturbations of the single site Metropolis and of the single cluster update schemes. Both the original algorithms (used to estimate some universal FSS curves of the XY universality class, see Sec. III) and the perturbed ones have been implemented in C language using double precision arithmetic.

Let us start from the perturbations of the single site Metropolis update. The essential step of this algorithm is the accept/reject step (sometimes called Metropolis filter) in Eq. (3), so we consider perturbations corresponding to “wrong” estimates of the energy difference  $\Delta E$ . A simple stochastic perturbation is obtained by considering in Eq. (3) the substitution

$$\Delta E \rightarrow \Delta E + G'_\sigma - G_\sigma, \quad (6)$$

where  $G'_\sigma$  and  $G_\sigma$  are two independent Gaussian random variables with zero average and variance  $\sigma^2$ . This perturbation can be thought of as a simple modeling of the case in which energies are not exactly computed but stochastically estimated. To mimic the effect of a finite machine precision we can instead use

$$\Delta E \rightarrow \text{round}(\Delta E \cdot \Lambda) / \Lambda, \quad (7)$$

where  $\text{round}(x)$  denotes the rounding to the closest integer of  $x$ , which amounts to truncate  $\Delta E$  with an accuracy  $1/\Lambda$ . To provide a scale for the values of  $\sigma$  and  $\Lambda$  used in the following section we note that the average value of  $\Delta E$  at the critical point of the XY model is  $\approx 2$ .

In the case of the single cluster update we modify the probability of adding a new site to the cluster, see Eq. (5). A random perturbation is obtained by performing the substitution

$$(\mathbf{s}_i \cdot \mathbf{v})(\mathbf{s}_o \cdot \mathbf{v}) \rightarrow (\mathbf{s}_i \cdot \mathbf{v})(\mathbf{s}_o \cdot \mathbf{v}) + G_\sigma, \quad (8)$$

where once again  $G_\sigma$  is a random Gaussian variable with zero average and variance  $\sigma^2$ . A finite precision truncation is instead obtained by using the substitution

$$(\mathbf{s}_i \cdot \mathbf{v})(\mathbf{s}_o \cdot \mathbf{v}) \rightarrow \text{round}[(\mathbf{s}_i \cdot \mathbf{v})(\mathbf{s}_o \cdot \mathbf{v})\Lambda]/\Lambda, \quad (9)$$

where round has been defined below Eq. (7). At the transition point of the XY model the average value of the quantity  $(\mathbf{s}_i \cdot \mathbf{v})(\mathbf{s}_o \cdot \mathbf{v})$  is  $\approx 0.25$ .

Let us stress that the mere fact that the typical value of the control parameter is smaller for the single cluster update than for the single site Metropolis update does not imply that the local update is more robust than the cluster one. The two update algorithms are so different from each other that it is not possible to draw such a conclusion based on this fact alone.

### III. NUMERICAL RESULTS

#### A. Observables and Finite Size Scaling

The observables we study can be defined starting from the two point correlation function of the spin:

$$G(\mathbf{x} - \mathbf{y}) = \langle \mathbf{s}_x \cdot \mathbf{s}_y \rangle. \quad (10)$$

In particular we consider Renormalization Group (RG) invariant observables, since the form of their FSS is particularly simple and allows for easy comparison between different models. The two RG invariant quantities considered are the Binder cumulant

$$U = \frac{\langle \mu_2^2 \rangle}{\langle \mu_2 \rangle^2}, \quad \mu_2 = \frac{1}{L^6} \sum_{\mathbf{x}, \mathbf{y}} \mathbf{s}_x \cdot \mathbf{s}_y, \quad (11)$$

and the ratio

$$R_\xi = \xi/L, \quad (12)$$

where the second moment correlation length  $\xi$  is defined by

$$\xi^2 = \frac{1}{4 \sin^2(p_{\min}/2)} \frac{\tilde{G}(\mathbf{0}) - \tilde{G}(\mathbf{p})}{\tilde{G}(\mathbf{p})}. \quad (13)$$

In this expression  $p_{\min} = 2\pi/L$  is the minimum non-vanishing momentum consistent with periodic boundary conditions,  $\mathbf{p} = (p_{\min}, 0, 0)$ , and  $\tilde{G}(\mathbf{k})$  is the Fourier transform of the two point correlation function  $G(\mathbf{x})$  computed at momentum  $\mathbf{k}$ .

$\beta_c$	0.45416474(10)[7]
$\nu$	0.67169(7)
$\omega$	0.789(4)
$R_\xi^*$	0.59238(7)
$U^*$	1.24296(8)

TABLE I: Critical temperature and (some) universal critical properties of the XY model, from [38] (see, e.g., [33–37, 39–41] for other determinations).

If we introduce the standard notation  $\tau = (\beta - \beta_c)/\beta_c$ , the FSS of a generic RG invariant quantity  $R$  can be written in the form (see, e. g., [17])

$$R(\beta, L) \simeq \mathcal{R}(L^{1/\nu}\tau) + L^{-\omega}\mathcal{R}_\omega(L^{1/\nu}\tau) + \dots. \quad (14)$$

In this expression  $\nu$  is the critical exponent related to the divergence at  $\beta = \beta_c$  of the correlation length in the thermodynamic limit,  $\omega > 0$  is (up to a sign) the scaling dimension of the first irrelevant operator at the transition, and the final dots stand for further irrelevant contributions and analytic background terms.  $\mathcal{R}$  is a scaling function universal up to a rescaling of its argument, while  $\mathcal{R}_\omega$  is universal up to a multiplicative constant and up to a rescaling of its argument, as can be seen starting from the standard scaling form of free energy density (see, e.g., [17]). In particular it follows that

$$\lim_{L \rightarrow \infty} R(\beta_c, L) = \mathcal{R}(0) \quad (15)$$

is universal. For the convenience of the reader we report in Tab. I the universal values the observables  $R_\xi$  and  $U$  (denoted by an asterisk) and of the critical exponents  $\nu$  and  $\omega$  for the three dimensional XY universality class, as well as the value of the critical temperature  $\beta_c$  for the XY model.

Since  $R_\xi$  turns out to be a monotonically increasing function of  $\beta$  (and thus of  $\tau$ ), it is possible to invert the relation  $\tau \rightarrow R_\xi$  and rewrite the FSS for  $U$  as a function of  $R_\xi$ :

$$U(\beta, L) = \mathcal{U}(R_\xi) + L^{-\omega}\mathcal{U}_\omega(R_\xi) + \dots. \quad (16)$$

In this expression  $\mathcal{U}$  is a universal scaling function independent of any non-universal rescaling factor, while  $\mathcal{U}_\omega$  is still universal only up to a multiplicative constant. Verifying that Eq. (16) holds with the same asymptotic scaling curve  $\mathcal{U}(R_\xi)$  is thus a particularly convenient way of testing whether two different models are in the same universality class.

#### B. XY scaling curve

Since the function  $\mathcal{U}(R_\xi)$  entering Eq. (16) is universal, it will be useful in the following to have a parametric representation of it, to investigate whether the results

$b_0$	-17.46924088170859	$c_0$	10.70348785915293
$b_1$	0.66215088251974	$c_1$	0.37099210816252
$b_2$	-0.82048697561210	$c_2$	-0.42383845323376
$b_3$	13.78704076975388	$c_3$	-10.06615359507961
$b_4$	3.85932964105796	$c_4$	-1.31489275164629
$b_5$	-1.29662539205099	$c_5$	0.59437782721002

TABLE II: Optimal fit parameters obtained by fitting data for  $U(R_\xi)$  of the XY model in the interval  $R_\xi \in [0.3, 1]$  using the parametrization in Eqs. (17)-(18). To perform the fit we only consider lattices with  $L \geq 16$ .

obtained using the perturbed models display the same critical behavior of the original XY model.

To parametrize  $U(R_\xi)$  in the XY model we use the same functional form already adopted in [48]

$$f(x) = 2 + a_0 x^2 (1 - e^{-8x^2}) - (a_1 + a_2 x)(1 - e^{-7x^2}) + \sum_{i=3}^5 a_i x^{i-1}, \quad (17)$$

where the coefficients  $a_i$  have a  $L$  dependence which takes into account the leading scaling corrections

$$a_k = b_k + L^{-\omega} c_k. \quad (18)$$

We simulated several values of  $\beta$  for  $L = 8, 16, 24, 32, 50, 64,$  and  $80$ , and performed the fit to Eq. (17) on the interval  $0.3 \leq R_\xi \leq 1$ , using only data coming from lattices of linear extent  $L \geq 16$ . The optimal values obtained for the fit parameters are reported in Tab. II, and using a bootstrap procedure we estimated the average relative error of  $U(R_\xi)$  to be  $\approx 8 \times 10^{-5}$  (with the maximum relative error being  $\approx 2 \times 10^{-4}$ ), and the average relative error of  $U_\omega(R_\xi)$  to be  $\approx 0.013$  (with the maximum relative error being  $\approx 0.046$ ). Note that these values are just statistical errors, and do not take into account the systematics related to the choice of the fit function. We will come back to this point in a moment.

Numerical data for  $U$  as a function of  $R_\xi$  are shown in Fig. 1, together with the estimates of  $U(R_\xi)$  and  $U_\omega(R_\xi)$  obtained by the above described fit. In the upper panel of Fig. 1 a zoom is shown of the region corresponding to  $\beta \approx \beta_c$ , with dashed lines corresponding to the known values of the universal quantities  $R_\xi^*$  and  $U^*$  (see Tab. I). Using  $R_\xi^* = 0.59238$  we obtain for  $U^*$  the estimate  $f(R_\xi^*) = 1.24306(11)$  which is nicely consistent with the known value  $1.24296(8)$  obtained in Ref. [38] and reported in Tab. I. This is a good indication that systematic errors related to the fitting procedure are likely smaller than the statistical ones, at least for  $U(R_\xi)$  and  $R_\xi \approx R_\xi^*$ .

In the lower panel of Fig. 1 we also show results related to the numerical estimate of  $U_\omega(R_\xi)$ , from which it can be seen that data obtained from the  $L = 8$  lattice systematically deviate from the other ones; this is why we included only  $L \geq 16$  data in the fit. For what concerns

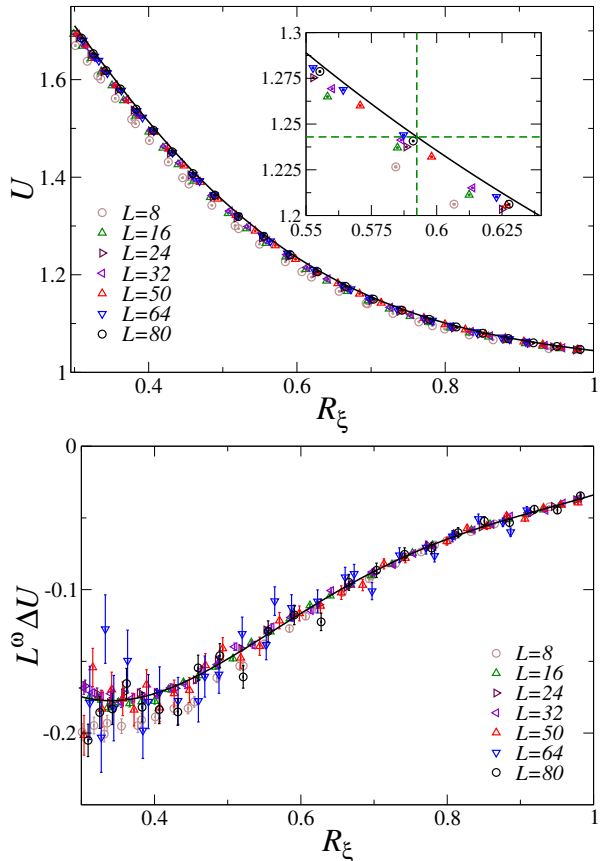


FIG. 1: Numerical estimates of the scaling curves  $U(R_\xi)$  and  $U_\omega(R_\xi)$  (see Eq. (16)) of the XY model. (upper panel) Numerical results for  $U$  as a function of  $R_\xi$ . The solid line is the result of the fit to Eqs. (17)-(18) described in the main text. The inset shows a zoom of the region corresponding to  $\beta \approx \beta_c$ , and dashed lines are drawn in correspondence of the known universal values  $R_\xi^*$  and  $U^*$ , see Tab. I, which have not been used in the fitting procedure. (lower panel) Numerical results for  $L^\omega(U(R_\xi) - U(R_\xi^*)) \approx U_\omega(R_\xi)$ , computed by using the value of the leading correction exponent reported in Tab. I. The solid line is the result of the fit to Eqs. (17)-(18) described in the main text.

the systematic errors of the  $U_\omega(R_\xi)$  determination, we expect them to be larger than those affecting  $U(R_\xi)$ , but we have not data to quantify them in a robust way. For this reason, in the following analyses of the perturbed models, we will just use  $U(R_\xi)$ , and in particular the fact that  $(U - U(R_\xi))L^\omega$  converges to a scaling curve, without explicitly comparing this scaling curve with the estimate of  $U_\omega(R_\xi)$  obtained from the XY model. Of course we could also directly compare data reported in the lower panel of Fig. 1 with the corresponding data of the perturbed model, but we would anyway have to fix the value of a non-universal parameter, see Sec. III A. Since however statistical errors of the quantity  $(U - U(R_\xi))L^\omega$  will turn out to be quite large for the perturbed models, the result of this comparison (although positive) is not particularly significant, and will not be reported in the following.

$\sigma^2$	$\beta_c(R)$	$\beta_c(U)$
0.01	0.4548716(65)	0.454884(15)
0.1	0.4613098(46)	0.461329(19)
1	0.533932(11)	0.533967(19)

TABLE III: Single site Metropolis update with Gaussian random energy perturbation (see Eq. (6)): estimates of the critical temperature for different values of  $\sigma^2$ , obtained by analyzing  $R_\xi$  or  $U$ . For comparison the critical temperature of the XY model is 0.45416474(10)[7] (from Ref. [38]).

$\Lambda$	$\beta_c(R)$	$\beta_c(U)$
$10^3$	0.4542428(83)	0.4542441(55)
10	0.4621358(86)	0.462136(13)
2	0.498336(10)	0.498350(15)

TABLE IV: Single site Metropolis update with energy truncation perturbation (see Eq. (7)): estimates of the critical temperature for different values of  $\Lambda$ , obtained by analyzing  $R_\xi$  or  $U$ . For comparison the critical temperature of the XY model is 0.45416474(10)[7] (from Ref. [38]).

### C. Perturbed MCMC results

#### 1. Single site Metropolis algorithm

We now present the results obtained by using the perturbed single site Metropolis update to sample the configurations of the three dimensional XY model.

Let us start from the stochastic perturbation described by Eq. (6), in which a Gaussian noise with zero average and variance  $\sigma^2$  is added to the energies of the configurations. We considered three values of the variance ( $\sigma^2 = 0.01, 0.1, 1$ ), and for each value of  $\sigma^2$  we performed simulation at several values of  $\beta$  using four different lattice sizes ( $L = 8, 16, 24, 32$ ).

To quantify the effect of the perturbation on non-universal quantities, for each value of  $\sigma^2$  we estimate the critical temperature from the crossing points of  $R_\xi$  and  $U$  as a function of  $\beta$ . More precisely, we use the FSS reported in Eq. (14), with polynomial approximations of the functions  $\mathcal{R}(x)$  and  $\mathcal{R}_\omega(x)$ , to fit data. In all the cases we fix  $\nu$ ,  $\omega$ ,  $R_\xi^*$  and  $U^*$  using the universal values of the XY universality class reported Tab. I. Already the fact that the fit used to extract  $\beta_c$  results in a  $\chi^2/\text{dof} \approx 1$  is thus a first indication that universal quantities are not affected by the stochastic noise. The residual dependence of the results on the degree of the polynomials used in the fit, or on the fit range adopted, has been added as a systematic error to the statistical error, and the final results are reported in Tab. III. The good agreement between the estimates obtained using  $R_\xi$  and those obtained using  $U$  is an indication that systematical errors have been correctly taken into account.

We discuss in detail just the case of the largest perturbation considered (i. e.  $\sigma^2 = 1$ ), since the conclusions are

the same also for the other values of  $\sigma^2$  investigated. In Fig. 2 (upper panel) we show data for  $R_\xi$  as a function of the scaling variable  $(\beta - \beta_c)L^{1/\nu}$ , obtained by using the result reported in Tab. III for  $\beta_c$  and the known value of the XY critical exponent  $\nu$ . The almost perfect scaling is a strong indication that universal quantities are unaffected by this perturbation of the MCMC algorithm.

The same conclusion can be reached from the scaling of  $U$  as a function of  $(\beta - \beta_c)L^{1/\nu}$  (not shown), and also by looking at the scaling  $U$  against  $R_\xi$ , shown in Fig. 2 (lower panel). It is indeed quite clear that data are approaching the universal XY curve  $\mathcal{U}(R_\xi)$  previously determined in Sec. IIIB. To better appreciate this fact we report in Fig. 3 data for  $L^\omega(U - \mathcal{U}(R_\xi))$ , obtained by using the known XY value of the leading correction to scaling exponent  $\omega$  (see Tab. I) and the universal XY curve  $\mathcal{U}(R_\xi)$ . The fact that data asymptotically (i. e. for large  $L$ ) approach a common scaling curve implies both

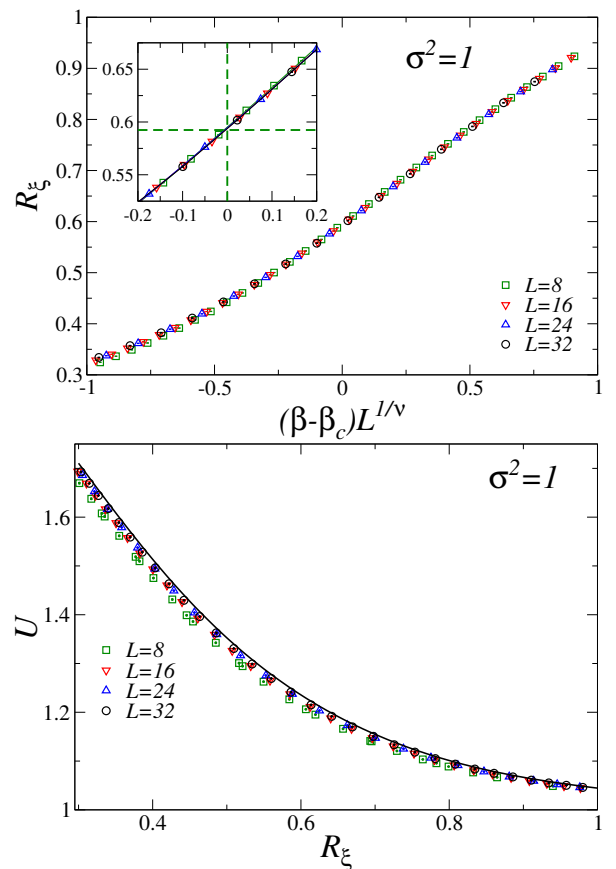


FIG. 2: Results for the single site Metropolis update with Gaussian random energy perturbation (see Eq. (6)) with variance  $\sigma^2 = 1$ . (upper panel) FSS of  $R_\xi$  obtained by using the value of the critical temperature reported in Tab. III and the value of the critical exponent  $\nu$  reported in Tab. I. The inset shows a zoom of the region close to  $\beta \approx \beta_c$ , and dashed lines are drawn in correspondence of  $\beta = \beta_c$  and  $R_\xi = R_\xi^*$ . (lower panel) Scaling of  $U$  against  $R_\xi$ . The solid line is the parametrization of the universal scaling curve  $\mathcal{U}(R_\xi)$  of the XY model obtained in Sec. IIIB.

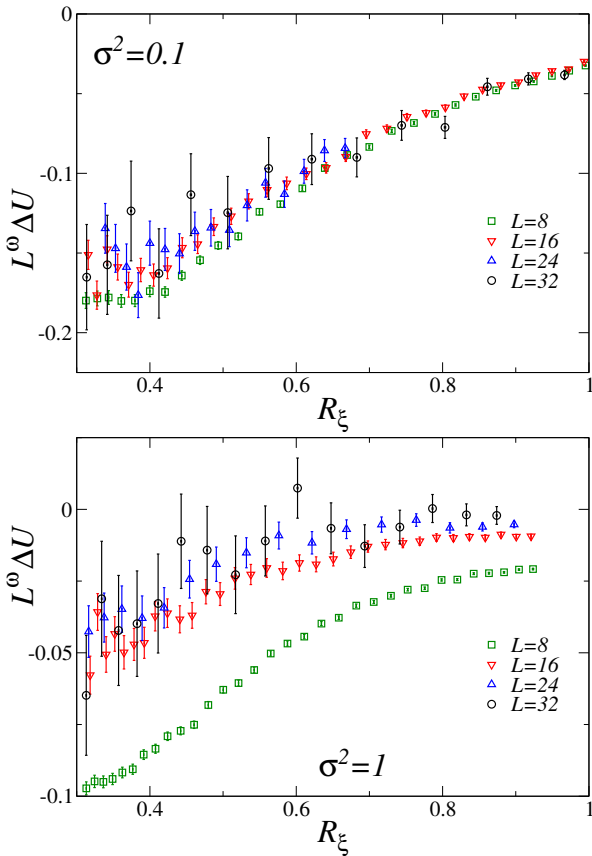


FIG. 3: Results for the single site Metropolis update with Gaussian random energy perturbation (see Eq. (6)). Estimates of  $L^\omega(U(R_\xi) - \mathcal{U}(R_\xi))$ , for the model with  $\sigma^2 = 0.1$  (upper panel) and  $\sigma^2 = 1$  (lower panel).

that  $\mathcal{U}(R_\xi)$  correctly describes the asymptotic behavior of  $U$  as a function of  $R_\xi$ , and that  $\omega = \omega_{XY}$  is the leading scaling correction exponent. It is interesting to note that the size of the leading corrections to scaling is actually reduced by increasing the value of variance  $\sigma^2$ , as can be seen from Fig. 3, where data for  $\sigma^2 = 0.1$  and  $\sigma^2 = 1$  are reported (note the different scale of the vertical axis in the two panels). This could explain why scaling corrections appear to be well described by the  $\mathcal{O}(L^{-\omega})$  behavior practically for all the values of  $L$  for  $\sigma^2 = 0.1$  but not for  $\sigma^2 = 1$ : since the size of the  $\mathcal{O}(L^{-\omega})$  corrections for  $\sigma^2 = 1$  is smaller than for  $\sigma^2 = 0.1$ , the effect of higher dimensional irrelevant operators becomes noticeable in the  $\sigma^2 = 1$  case.

A completely analogous analysis has been carried out also for the single site Metropolis update with the truncation error described by Eq. (6). Also in this case we considered three values of the cut-off  $\Lambda$  ( $\Lambda = 10^3, 10, 2$ ), and for each value of  $\Lambda$  we performed simulation at several values of  $\beta$  using four different lattice sizes ( $L = 8, 16, 24, 32$ ).

The critical temperature has been estimated, for the different values of the cut-off  $\Lambda$  investigated, using the same procedure described above, and the final results

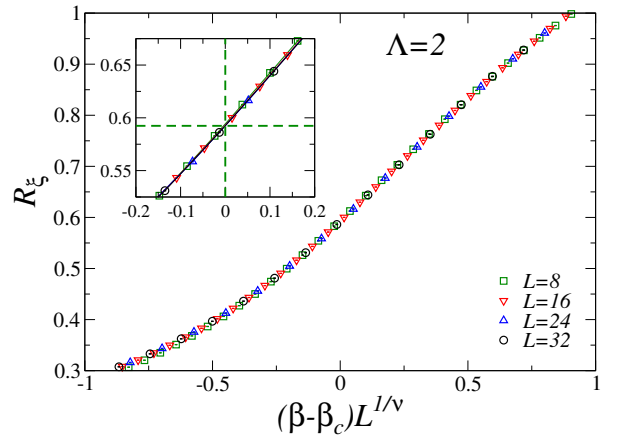


FIG. 4: Results for the single site Metropolis update with truncation energy perturbation (see Eq. (7)) with truncation cut-off  $\Lambda = 2$ . FSS of  $R_\xi$  obtained by using the value of the critical temperature reported in Tab. IV and the value of the critical exponent  $\nu$  reported in Tab. I. The inset shows a zoom of the region close to  $\beta \approx \beta_c$ , and dashed lines are drawn in correspondence of  $\beta = \beta_c$  and  $R_\xi = R_\xi^*$ .

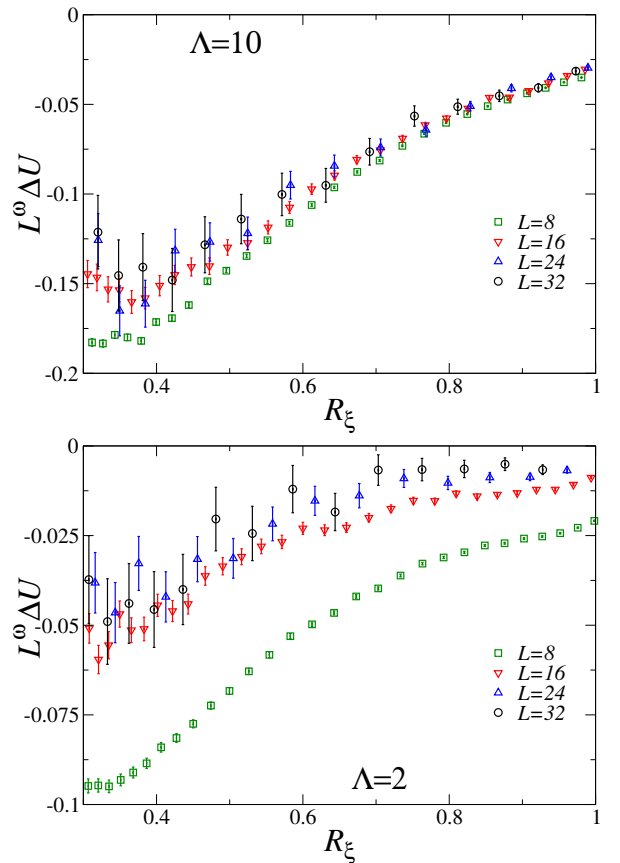


FIG. 5: Results for the single site Metropolis update with truncation energy perturbation (see Eq. (7)). Estimates of  $L^\omega(U(R_\xi) - \mathcal{U}(R_\xi))$ , for the model with  $\Lambda = 10$  (upper panel) and  $\Lambda = 2$  (lower panel).

$\sigma^2$	$\beta_c(R)$	$\beta_c(U)$
0.1	0.4887867(44)	0.4887893(55)
0.5	0.608378(17)	0.608361(24)

TABLE V: Single cluster update with Gaussian random energy perturbation of the cluster formation probability (see Eq. (8)): estimates of the critical temperature for different values of  $\sigma^2$ , obtained by analyzing  $R_\xi$  or  $U$ . For comparison the critical temperature of the XY model is 0.45416474(10)[7] (from Ref. [38]).

$\Lambda$	$\beta_c(R)$	$\beta_c(U)$
$10^3$	0.4545794(11)	0.4545782(10)
$10^2$	0.4583497(15)	0.4583490(15)
10	0.5004(2)	0.5007(2)

TABLE VI: Single cluster update with truncation perturbation of the cluster formation probability (see Eq. (9)): estimates of the critical temperature for different values of  $\Lambda$ , obtained by analyzing  $R_\xi$  or  $U$ . For comparison the critical temperature of the XY model is 0.45416474(10)[7] (from Ref. [38]).

are reported in Tab. IV. Also in this case the scaling of  $R_\xi$  as a function of  $(\beta - \beta_c)L^{1/\nu}$ , obtained by fixing the value of  $\nu$  corresponding to the XY universality class, is extremely good even for the huge value  $\Lambda = 2$  of the cut-off, as can be seen from Fig. 4.

A further check of the XY nature of the critical behavior is provided by the scaling of  $U$  as a function of  $R_\xi$ : also in this case data converge to the universal curve  $\mathcal{U}(R_\xi)$  of the XY model determined in Sec. III B, and in Fig. 5 we report the results for  $L^\omega(U(R_\xi) - \mathcal{U}(R_\xi))$ . The fact that numerical results for this quantity asymptotically (in the  $L \rightarrow \infty$  limit) collapse on a scaling curve ensures that  $U(R_\xi)$  is effectively converging to the universal XY scaling function  $\mathcal{U}(R_\xi)$  with  $O(L^{-\omega})$  corrections. By comparing the results reported in Fig. 5 for  $\Lambda = 10$  and  $\Lambda = 2$  (note the different scale on the vertical axis in the two panels) we can see that by decreasing  $\Lambda$ , i. e. by increasing the size of the truncation error, the size of the leading corrections to scaling decreases, which is the equivalent in the present case of what already noted when discussing the stochastic perturbation of the single site Metropolis algorithm.

## 2. Single cluster update

Let us now discuss how MCMC perturbations affect the result obtained by using the single cluster algorithm. We start again from the stochastic perturbation case, and in the cluster algorithm the perturbation involves the acceptance probability to be used in building the cluster. In particular we consider the Gaussian perturbation in Eq. (8) of the standard acceptance probability Eq. (5), with zero average and variance  $\sigma^2$ . In this case we con-

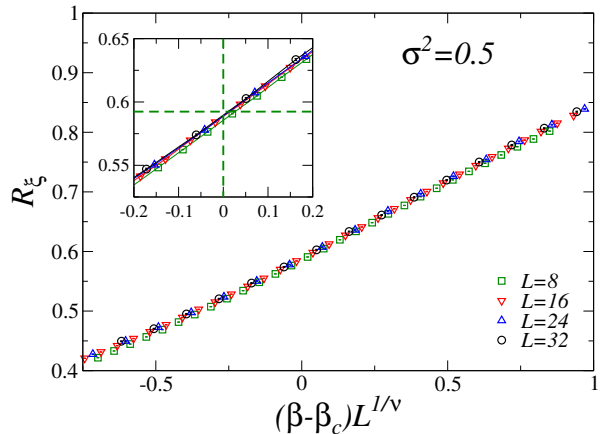


FIG. 6: Results for the single cluster update with Gaussian random perturbation (see Eq. (8)) with variance  $\sigma^2 = 0.5$ . FSS of  $R_\xi$  obtained by using the value of the critical temperature reported in Tab. V and the value of the critical exponent  $\nu$  reported in Tab. I. The inset shows a zoom of the region close to  $\beta \approx \beta_c$ , and dashed lines are drawn in correspondence of  $\beta = \beta_c$  and  $R_\xi = R_\xi^*$ .

sidered two values of the variance ( $\sigma^2 = 0.1, 0.5$ ), and for each value of  $\sigma^2$  we performed simulations for several  $\beta$  values, using lattices of linear extent  $L = 8, 16, 24, 32$ .

Critical temperatures have been determined using the same procedure described when discussing the single site Metropolis perturbations, and the final results obtained in this way are reported in Tab. V. Deviations of the critical temperatures in Tab. V from the  $\beta_c$  value of the unperturbed XY model are larger than for the previously studied perturbations (see Tabs. III, IV), however the critical behavior turns out to be still consistent with that of the three dimensional XY universality class.

In Fig. 6 we report  $R_\xi$  data as a function of  $(\beta - \beta_c)L^{1/\nu}$  for the case  $\sigma^2 = 0.5$ , where  $\beta_c$  can be read from Tab. V and for  $\nu$  we used the XY universality class value in Tab. I. Some slight scaling corrections are present in data computed on the  $L = 8$  lattice, but overall the data collapse is still very good on larger lattices, and a similar picture emerges from the analysis of  $U$  data as a function of  $(\beta - \beta_c)L^{1/\nu}$  (not shown).

Results for  $L^\omega(U(R_\xi) - \mathcal{U}(R_\xi))$  as a function of  $R_\xi$  are shown in Fig. 7 for the values  $\sigma^2 = 0.1$  and  $\sigma^2 = 0.5$  of the noise variance. These data clearly show that the universal scaling function  $\mathcal{U}(R_\xi)$  correctly describes the asymptotic FSS behavior of  $U$  as a function of  $R_\xi$ , with  $O(L^{-\omega})$  corrections and  $\omega = \omega_{XY}$ , thus further confirming that the observed critical behavior is consistent with that of the XY universality class. For the cluster update with a stochastic perturbation also the size of the scaling corrections is almost independent of the variance  $\sigma^2$ , as can be seen by comparing data in Fig. 7 with those in Fig. 1 (lower panel). It is however important to stress that errors do change with the value of  $\sigma^2$ : data reported in the two panels of Fig. 7 have been obtained using similar statistics (differing at most by a factor of 2) but the

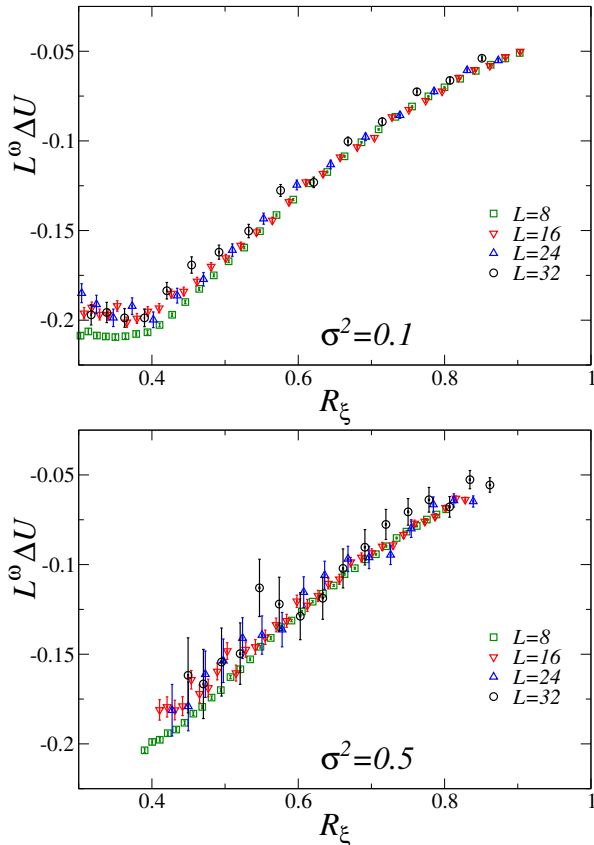


FIG. 7: Results for the single cluster update with Gaussian random perturbation (see Eq. (8)). Estimates of  $L^\omega(U(R_\xi) - \mathcal{U}(R_\xi))$ , for the model with  $\sigma^2 = 0.1$  (upper panel) and  $\sigma^2 = 0.5$  (lower panel).

errors observed for  $\sigma^2 = 0.5$  are much larger than what could be expected by rescaling the errors for  $\sigma^2 = 0.1$ . This is an indication of the fact that the perturbation is not strong enough to break down the algorithm (the correct universal critical behavior is still observed) but the correlation between the clusters identified by the algorithm and the relevant critical modes decreases as  $\sigma^2$  is increased.

Let us finally consider the case of the single cluster update with a truncation error in the probability of adding a site to the cluster, see Eq. (9). To study this case we considered three values of the cut-off  $\Lambda$  ( $\Lambda = 10^3, 10^2, 10$ ), and for each value of  $\Lambda$  we performed simulations for several  $\beta$  values, using lattices of linear extent going from  $L = 8$  up to  $L = 60$ .

For  $\Lambda = 10^3$  and  $\Lambda = 10^2$  it was possible to carry out the analysis as done in the previous cases: the critical temperatures have been estimated by performing biased fits of  $R_\xi$  and  $U$  data, using polynomial approximations of the FSS relation Eq. (14) with the constants  $\nu, \omega, R_\xi^*$  and  $U^*$  fixed to the universal XY values reported in Tab. I. The final results for the critical temperatures obtained in this way are reported in Tab. VI. For both the  $\Lambda = 10^3$  and  $\Lambda = 10^2$  cases the critical behavior is

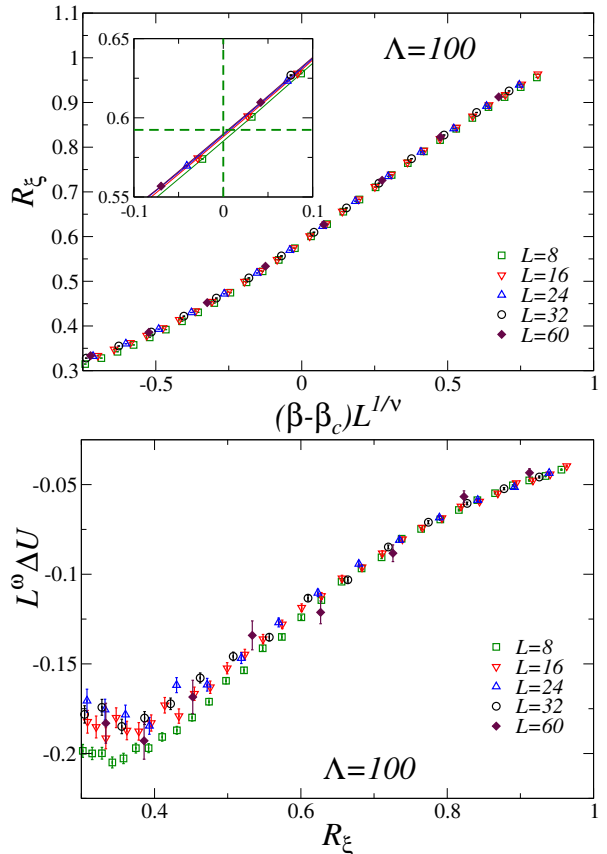


FIG. 8: Results for the single cluster update with truncation energy perturbation (see Eq. (9)) and  $\Lambda = 100$ . (upper panel) FSS of  $R_\xi$  obtained by using the value of the critical temperature reported in Tab. VI and the value of the critical exponent  $\nu$  reported in Tab. I. The inset shows a zoom of the region close to  $\beta \approx \beta_c$ , and dashed lines are drawn in correspondence of  $\beta = \beta_c$  and  $R_\xi = R_\xi^*$ . (lower panel) Estimates of  $L^\omega(U(R_\xi) - \mathcal{U}(R_\xi))$ , with  $\omega = \omega_{XY}$ , see Tab. I.

fully consistent with the standard XY universality class. Results for  $\Lambda = 10^2$  are shown in Fig. 8, from which it is clear that  $R_\xi$  scales with  $(\beta - \beta_c)L^{1/\nu}$ ,  $\nu = \nu_{XY}$ , and that the asymptotic behavior of  $U$  as a function of  $R_\xi$  is consistent with the scaling function  $\mathcal{U}(R_\xi)$  determined in Sec. III B.

The case  $\Lambda = 10$  is the only one in which biased fits to extract the critical temperature were not able to correctly reproduce the behavior of  $R_\xi$  and  $U$  data. From Fig. 9 (upper panel) it is indeed quite clear that the crossing point of  $R_\xi$  data is different from the value  $R_\xi^*$  reported in Tab. I. Analogously, the XY scaling curve  $\mathcal{U}(R_\xi)$  does not describe the asymptotic behavior of  $U$  as function of  $R_\xi$ , as can be clearly seen from the lower panel of Fig. 9. For  $\Lambda = 10$  the transition is thus definitely not in the three dimensional XY universality class.

The values of the critical temperature reported in Tab. VI for the case  $\Lambda = 10$  have been obtained by performing unbiased fits of  $R_\xi$  and  $U$ , i. e. using the values of  $\nu, R_\xi^*$  and  $U^*$  as fit parameters, and considering sev-

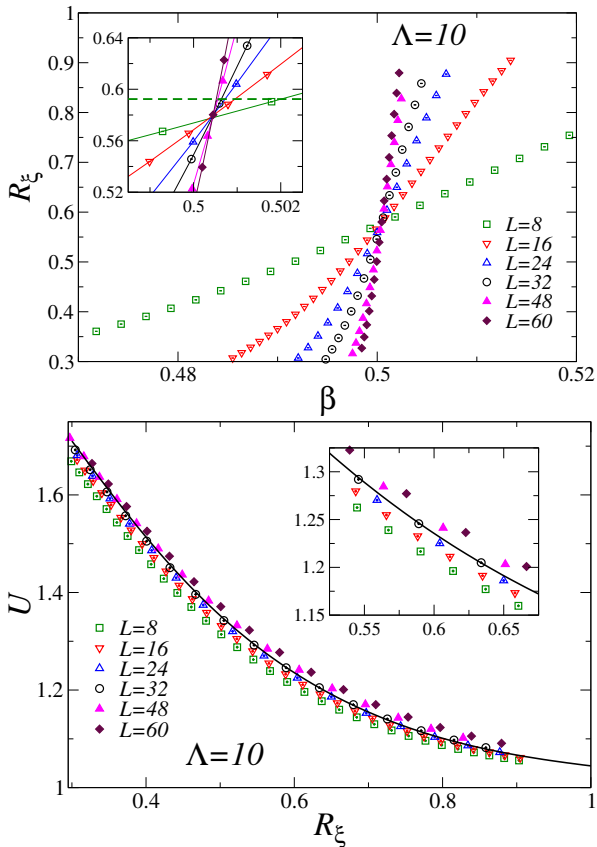


FIG. 9: Results for the single cluster update with truncation energy perturbation (see Eq. (9)) and  $\Lambda = 10$ . (upper panel) Data for  $R_\xi$ ; in the inset a zoom of the  $\beta \approx \beta_c$  region is shown, and the horizontal dashed line is drawn in correspondence of the universal XY critical value  $R_\xi^*$  reported in Tab. I. (lower panel) Data for  $U$  against  $R_\xi$ , plotted together with the universal scaling curve  $U(R_\xi)$  of the XY model obtained in Sec. III B.

eral values of  $\omega$  in the range  $[0, 1]$ . These fits did not provided us with a solid estimate of the critical exponent  $\nu$ , which drift from  $\approx 0.7$  to  $\approx 0.9$  when data obtained on small  $L$  lattices are excluded from the fit. All these facts together contribute to make the estimates of  $\beta_c$  in this case much less accurate than in the other cases.

#### IV. CONCLUSIONS

We investigated the stability of the universal properties at continuous phase transitions against perturbations of the MCMC algorithm, considering both local and global update schemes, and stochastic and deterministic perturbations.

For the case of the classical three dimensional XY model, which we used as test bed for this investigation, we found universal properties to be surprisingly stable, even against very large perturbations. Indeed in all but one case critical exponents and universal scaling curves have been unaffected, within the statistical accuracy, by

the introduction of perturbations so large as to modify the second significant figure of the energy.

It is natural to interpret such a stability as due to the presence of “universality classes” of MCMC algorithms, however the development of an appropriate RG framework to handle these type of perturbation is obviously required to put this interpretation on solid ground. Note that the framework required is different from that of critical dynamics [43, 44]: for what concerns the stability against perturbations local and global algorithms appear to behave in an analogous way, although they definitely have different critical dynamical properties (and in particular different values of the dynamic critical exponent  $z$ ). Despite all these precautions it is difficult not to state that the perturbations considered in this work are irrelevant in a RG-like sense.

To further corroborate this interpretation of the numerical results more investigations are clearly required, to check if a similar phenomenology is observed also using different statistical models. It would in particular be interesting to understand what happens at charged transitions in gauge theories [49], since perturbations of the dynamics could result in soft breaking of the gauge invariance.

Another possibility for further studies is the characterization of the critical behavior emerging when the perturbation changes the universality class of the transition. We could identify only one case in which this happens, i. e. the single cluster update with a very large truncation error, but large scaling corrections prevented us from characterizing the critical properties in this case. In particular we have no hints if the critical behavior observed corresponds to an already known universality class or to something new.

For classical simulations performed on standard CPUs the topic investigated in this work is probably important mainly from the theoretical point of view, but it can be of more direct practical relevance in the context of quantum algorithms, or even to speed-up simulations using low-accuracy hardware.

#### Acknowledgments

It is a pleasure to thank Francesco Grotto and Silvia Morlacchi for useful discussions. C.B. acknowledge support from the project PRIN 2022 “Emerging gauge theories: critical properties and quantum dynamics” (20227JZKWP). This study was carried out within the National Centre on HPC, Big Data and Quantum Computing - SPOKE 10 (Quantum Computing) and received funding from the European Union Next-GenerationEU - National Recovery and Resilience Plan (NRRP) – MISSION 4 COMPONENT 2, INVESTMENT N. 1.4 – CUP N. I53C22000690001. Numerical simulations have been performed on the CSN4 cluster of the Scientific Computing Center at INFN-PISA.

- 
- [1] R. J. Baxter, *Exactly Solved Model in Statistical Mechanics* (Academic Press, London, UK, 1982).
- [2] C. Itzykson and J.-M. Drouffe, *Statistical field theory* (Cambridge University Press, Cambridge, UK, 1991).
- [3] B. M. McCoy, *Advanced Statistical Mechanics* (Oxford University Press, Oxford, UK, 2010).
- [4] M. E. J. Newman and G. T. Barkema, *Monte Carlo Methods in Statistical Physics* (Clarendon Press, Oxford, UK, 2001).
- [5] K. Binder and D. W. Heermann, *Monte Carlo Simulations in Statistical Physics. An Introduction* (Springer, Berlin, Germany, 2002).
- [6] B. A. Berg, *Markov Chain Monte Carlo Simulations and Their Statistical Analysis* (World Scientific, Singapore, 2004).
- [7] D. P. Landau and K. Binder, *A Guide to Monte Carlo Simulations in Statistical Physics* (Cambridge University Press, Cambridge, UK, 2005).
- [8] W. Krauth, *Statistical Mechanics: Algorithms and Computations* (Oxford University Press, Oxford, UK, 2006).
- [9] M. D’Elia, K. Langfeld and B. Lucini, *Stochastic Methods in Scientific Computing. From Foundations to Advanced Techniques* (CRC Press, Boca Raton, Florida, 2024).
- [10] E. Y. Loh, J. E. Gubernatis, R. T. Scalettar, S. R. White, D. J. Scalapino and R. L. Sugar, “Sign problem in the numerical simulation of many-electron systems”, *Phys. Rev. B* **41**, 9301 (1990).
- [11] M. Troyer and U. J. Wiese, “Computational complexity and fundamental limitations to fermionic quantum Monte Carlo simulations,” *Phys. Rev. Lett.* **94**, 170201 (2005) [arXiv:cond-mat/0408370 [cond-mat]].
- [12] O. Philipsen, “Lattice QCD at non-zero temperature and baryon density,” [arXiv:1009.4089 [hep-lat]].
- [13] G. Aarts, “Introductory lectures on lattice QCD at nonzero baryon number,” *J. Phys. Conf. Ser.* **706** (2016), 022004 [arXiv:1512.05145 [hep-lat]].
- [14] K. G. Wilson and J. Kogut, “The renormalization group and the  $\epsilon$  expansion,” *Phys. Rep.* **12**, 75 (1974).
- [15] M. E. Fisher, “The renormalization group in the theory of critical behavior,” *Rev. Mod. Phys.* **47**, 543 (1975).
- [16] S.-K. Ma, *Modern Theory of Critical Phenomena* (Westview Press, Boulder, Colorado, 1976).
- [17] A. Pelissetto and E. Vicari, “Critical Phenomena and Renormalization Group Theory,” *Phys. Rep.* **368**, 549 (2002).
- [18] J. Zinn-Justin, *Quantum Field Theory and Critical Phenomena* (Oxford University Press, Oxford, UK, 2002).
- [19] M. Creutz, *Quarks, gluons and lattices* (Cambridge University Press, Cambridge, UK, 1983).
- [20] I. Montvay and G. Münster, *Quantum Fields on a Lattice* (Cambridge University Press, Cambridge, UK, 1994).
- [21] H. J. Rothe, *Lattice Gauge Theories. An Introduction* (World Scientific, Singapore, 2005).
- [22] T. DeGrand and C. DeTar, *Lattice Methods for Quantum Chromodynamics* (World Scientific, Singapore, 2006).
- [23] C. Gattringer and C. B. Lang, *Quantum Chromodynamics on the Lattice. An Introductory Presentation* (Springer, Berlin, Germany, 2010).
- [24] G. O. Roberts, J. S. Rosenthal and P. O. Schwartz, “Convergence properties of perturbed Markov chains,” *J. Appl. Prob.* **35**, 1 (1998).
- [25] L. Breyer, G. O. Roberts and J. S. Rosenthal, “A note on geometric ergodicity and floating-point roundoff error,” *Stat. & Prob. Lett.* **53**, 123 (2001).
- [26] Y. Takahashi, “Markov chains with random transition matrices,” *Kodai Math. Sem. Rep.* **21**, 426 (1969).
- [27] R. Cogburn, “The Ergodic Theory of Markov Chains in Random Environment,” *Z. Wahrscheinlichkeitstheorie verw. Gebiete* **66**, 109 (1984).
- [28] K. Temme, T. J. Osborne, K. G. Vollbrecht, D. Poulin and F. Verstraete, “Quantum Metropolis Sampling,” *Nature* **471**, 87 (2011) [arXiv:0911.3635 [quant-ph]].
- [29] M. H. Yung and A. Aspuru-Guzik, “A quantum–quantum Metropolis algorithm,” *Proc. Nat. Acad. Sci.* **109**, 754 (2012).
- [30] G. Clemente, M. Cardinali, C. Bonati, E. Calore, L. Cosmai, M. D’Elia, A. Gabbana, D. Rossini, F. S. Schifano, R. Tripicciono and D. Vadicchino, “Quantum computation of thermal averages in the presence of a sign problem,” *Phys. Rev. D* **101**, 074510 (2020) [arXiv:2001.05328 [hep-lat]].
- [31] R. Aiudi, C. Bonanno, C. Bonati, G. Clemente, M. D’Elia, L. Maio, D. Rossini, S. Tirone and K. Zambello, “Quantum algorithms for the computation of quantum thermal averages at work,” *Phys. Rev. D* **108**, 114509 (2023) [arXiv:2308.01279 [quant-ph]].
- [32] E. Ballini, G. Clemente, M. D’Elia, L. Maio and K. Zambello, “Quantum computation of thermal averages for a non-Abelian  $D_4$  lattice gauge theory via quantum Metropolis sampling,” *Phys. Rev. D* **109**, 034510 (2024) [arXiv:2309.07090 [quant-ph]].
- [33] H. G. Ballesteros, L. A. Fernandez, V. Martin-Mayor and A. Munoz Sudupe, “Finite size effects on measures of critical exponents in  $d = 3$   $O(N)$  models,” *Phys. Lett. B* **387**, 125 (1996) [arXiv:cond-mat/9606203 [cond-mat]].
- [34] R. Guida and J. Zinn-Justin, “Critical exponents of the  $N$  vector model,” *J. Phys. A* **31**, 8103 (1998) [arXiv:cond-mat/9803240 [cond-mat.stat-mech]].
- [35] E. Burovski, J. Machta, N. Prokof’ev and B. Svistunov, “High Precision Measurement of the Thermal Exponent for the Three-Dimensional XY Universality Class,” *Phys. Rev. B* **74**, 132502, (2006) [arXiv:cond-mat/0507352 [cond-mat.stat-mech]].
- [36] M. Campostrini, M. Hasenbusch, A. Pelissetto and E. Vicari, “The Critical exponents of the superfluid transition in  $^4\text{He}$ ,” *Phys. Rev. B* **74**, 144506 (2006) [arXiv:cond-mat/0605083 [cond-mat.stat-mech]].
- [37] M. V. Kompaniets and E. Panzer, “Minimally subtracted six loop renormalization of  $O(n)$ -symmetric  $\phi^4$  theory and critical exponents,” *Phys. Rev. D* **96**, 036016 (2017) [arXiv:1705.06483 [hep-th]].
- [38] M. Hasenbusch, “Monte Carlo study of an improved clock model in three dimensions,” *Phys. Rev. B* **100**, 224517 (2019) [arXiv:1910.05916 [cond-mat.stat-mech]].
- [39] W. Xu, Y. Sun, J. P. Lv and Y. Deng, “High-precision Monte Carlo study of several models in the three-dimensional  $U(1)$  universality class,” *Phys. Rev. B* **100**, 064525 (2019) [arXiv:1908.10990 [cond-mat.stat-mech]].
- [40] S. M. Chester, W. Landry, J. Liu, D. Poland, D. Simmons-Duffin, N. Su and A. Vichi, “Carving out OPE space and precise  $O(2)$  model critical exponents,” *JHEP* **06**, 142 (2020) [arXiv:1912.03324 [hep-th]].

- [41] G. De Polsi, I. Balog, M. Tissier and N. Wschebor, Precision calculation of critical exponents in the  $O(N)$  universality classes with the nonperturbative renormalization group, *Phys. Rev. E* **101**, 042113 (2020) [arXiv:2001.07525 [cond-mat.stat-mech]].
- [42] W. Krauth, Event-chain Monte Carlo: foundations, applications, and prospects, *Frontiers in Physics* **9**, 663457 (2021) [arXiv:2102.07217 [cond-mat.soft]].
- [43] P. C. Hohenberg and B. I. Halperin, Theory of dynamic critical phenomena, *Rev. Mod. Phys.* **49**, 435 (1977).
- [44] R. Folk and G. Moser, Critical dynamics: A field-theoretical approach, *J. Phys. A: Math. Gen.* **39**, R207 (2006).
- [45] N. Metropolis, A. W. Rosenbluth, M. N. Rosenbluth, A. H. Teller and E. Teller, Equation of state calculations by fast computing machines, *J. Chem. Phys.* **21**, 1087 (1953).
- [46] U. Wolff, Collective Monte Carlo Updating for Spin Systems, *Phys. Rev. Lett.* **62**, 361 (1989).
- [47] S. L. Adler, Over-relaxation method for the Monte Carlo evaluation of the partition function for multiquadratic actions, *Phys. Rev. D* **23**, 2901 (1981).
- [48] C. Bonati, A. Pelissetto and E. Vicari, Lattice gauge theories in the presence of a linear gauge-symmetry breaking, *Phys. Rev. E* **104**, 014140 (2021) [arXiv:2106.02503 [hep-lat]].
- [49] C. Bonati, A. Pelissetto and E. Vicari, Three-dimensional Abelian and non-Abelian gauge Higgs theories, *Phys. Rept.* **1133**, 1 (2025) [arXiv:2410.05823 [cond-mat.stat-mech]].